GW-Gamma-Rays Delay
&
Afterglow Polarization

Ramandeep Gill

Institute of Radio Astronomy & Astrophysics
(UNAM)

FEET24 **Bormio, Italy** **Feb 28, 2024**

Gamma-ray burst progenitors as GW sources

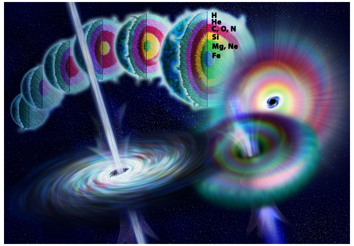

Progenitors of **long-GRBs** (T_{90} > 2 s) are massive ($M \geq 20 - 30\, M_{\odot}$) Wolf-Rayet stars that undergo core-collapse. (Woosley '93; Woosley & Bloom '06)

Short-GRBs (T_{90} < 2 s) are produced in the mergers of two NSs (e.g. GW170817) and NS + BH.
(Eichler+89; Narayan+92)

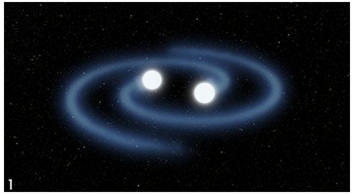

To lowest order, GWs are emitted when a rapidly changing mass distribution produces a time-varying quadrupole moment

GWs in the collapsar scenario

- Rotational instability in the central engine (Davies+02; Fryer+02; Kobayashi & Meszaros '03; Shibata+03; …)
- Estimates are still uncertain
- GW-gamma-ray delay can be up to few x 10s due to longer breakout times (Bromberg+12)

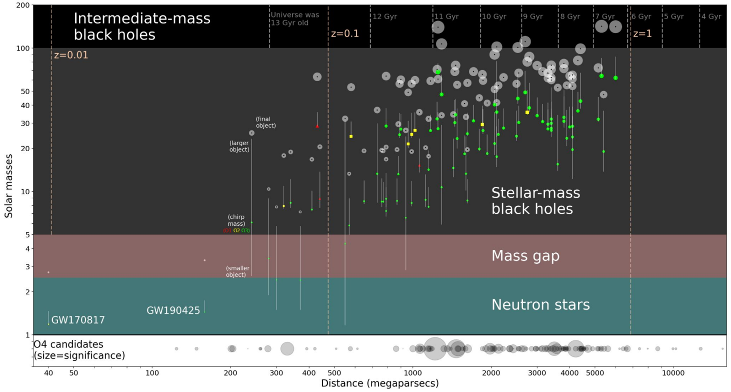

Gamma-ray burst progenitors as GW sources

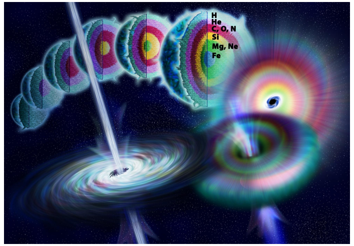

Progenitors of **long-GRBs** (T_{90} > 2 s) are massive ($M \geq 20 - 30\ M_{\odot}$) Wolf-Rayet stars that undergo core-collapse. (Woosley '93; Woosley & Bloom '06)

Short-GRBs (T_{90} < 2 s) are produced in the mergers of two NSs (e.g. GW170817) and NS + BH. (Eichler+89; Narayan+92)

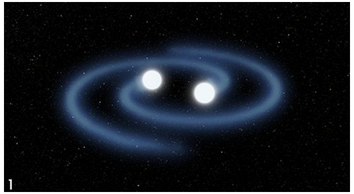

To lowest order, GWs are emitted when a rapidly changing mass distribution produces a time-varying quadrupole moment

GWs in the collapsar scenario

- Rotational instability in the central engine (Davies+02; Fryer+02; Kobayashi & Meszaros '03; Shibata+03; …)
- Estimates are still uncertain
- GW-gamma-ray delay can be up to few x 10s due to longer breakout times (Bromberg+12)

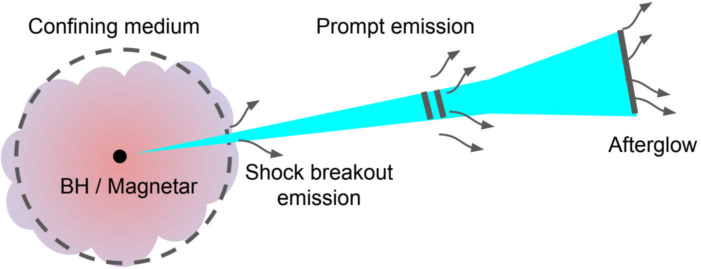

Why a delay between GWs and gamma-rays?

- Emission of gamma-rays is neither contemporaneous nor co-spatial with that of GWs:

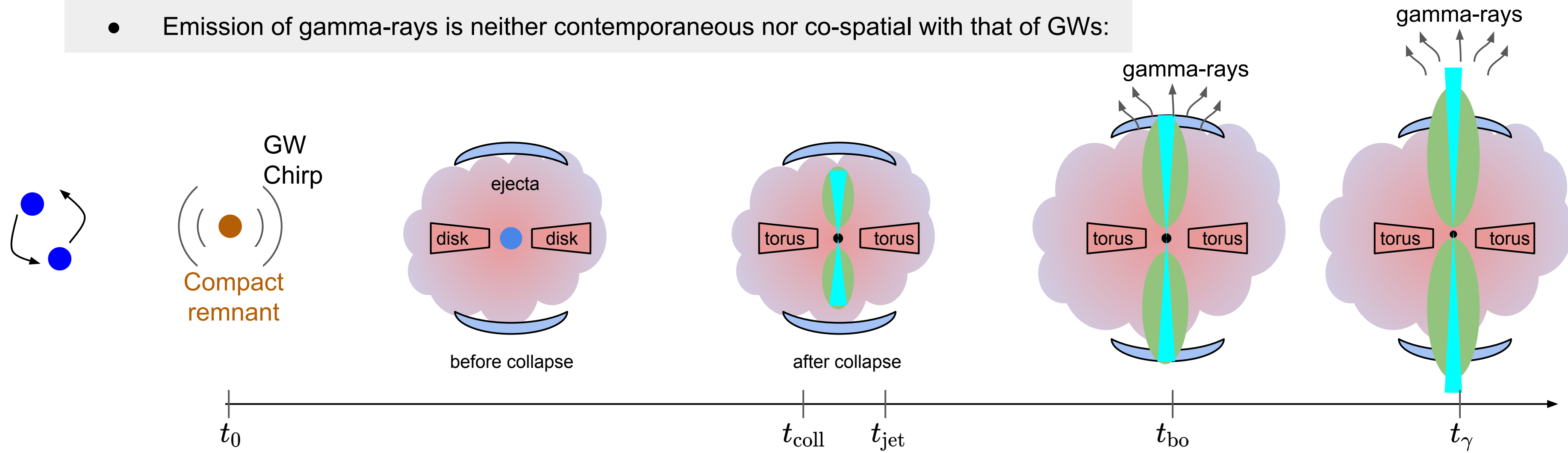

- Total delay w.r.t GW emission: $t_{\rm del} = [t_{\rm coll} + t_{\rm jet} + t_{\rm bo} + t_\gamma]\,(1+z)$

- Gravitons and gamma-ray photons move at different speeds:

$$t_{\rm del} = \frac{D}{c}\left(1 - \frac{c}{c_{\rm GW}}\right) \Rightarrow \left(1 - \frac{c}{c_{\rm GW}}\right) \simeq 4.2 \times 10^{-16} \left(\frac{D}{40\,{\rm Mpc}}\right)^{-1} \left(\frac{t_{\rm del}}{1.74\,{\rm s}}\right)$$

This delay can also be used to constrain the **Shapiro delay** that tests the **weak-equivalence principle** (e.g. LIGO-VIRGO-Fermi-INTEGRAL '17)

Merger remnant and collapse time

Stable NS: Long-lived NS, rapidly spinning, possibly with magnetar strength B-fields $\left(B_s \sim 10^{14-15}\mathrm{G}\right)$, that loses rotational energy due to magnetic dipole radiation on the spin-down time

$$\tau_{\rm sd} = \frac{Ic^3}{2f\Omega_0 R_{\rm NS}^6 B_0^2} \geq 3.4\times10^2 \frac{P_{0,-3}^2}{fB_{15}^2}\,\mathrm{s}$$

Supra-massive NS: Supported by rigid-body rotation; collapses to a BH on the spin-down time (if GW emission is sub-dominant):

$$t_{\rm coll} = \tau_{\rm sd} \qquad E_{\rm rot} = \frac{1}{2}I\Omega_0^2 \sim 10^{52.5-53}\,\mathrm{erg}$$

Hyper-massive NS: Supported by differential rotation; collapses to a BH on a much shorter timescale: (e.g. Kastaun & Galeazzi '15)

$$10^{-2}\mathrm{s} \leq t_{\rm coll} \leq 1\,\mathrm{s}$$

Prompt BH: BH forms directly if $M_{\rm tot} \geq 2.8 M_\odot$; mass of ejected matter is less

$$t_{\rm coll} = 0$$

GW170817 (Granot+17)

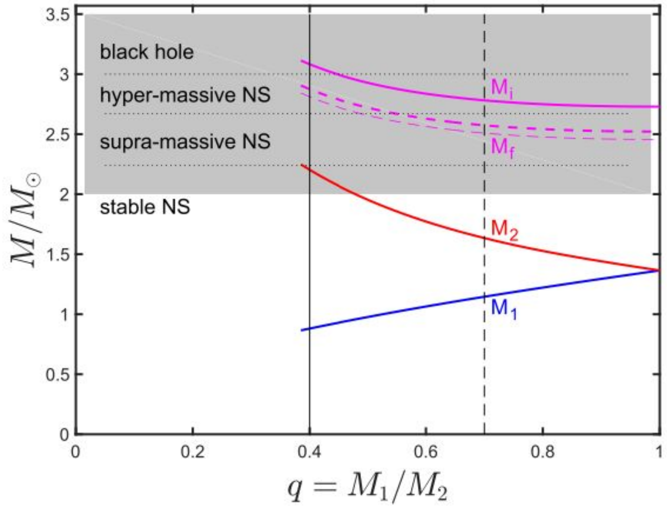

The **chirp mass** provides a strong constraint on the component masses for a given mass ratio:

$$\mathcal{M} = \frac{(M_1M_2)^{3/5}}{(M_1+M_2)^{1/5}} = M_2\frac{q^{3/5}}{(1+q)^{1/5}}$$

Ejecta in the path of the jet

NS + NS

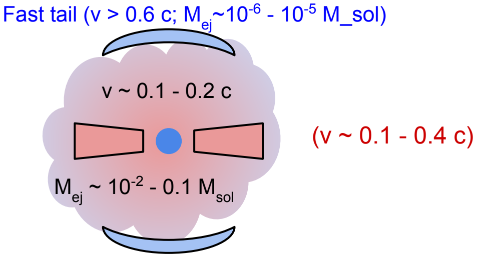

NS + BH

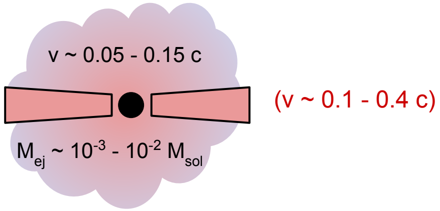

Before the compact remnant collapses to a BH, the external medium is polluted with ejecta from different channels: (see review by Nakar '19)

- **Dynamical ejecta** ($t < t_{dyn}$ ~ 10 ms):
  - **Tidal tails** (equatorial plane)
  - **shock-driven ejecta** (~ isotropic) - **only in NS+NS merger**
  - Depends strongly on EOS and mass ratio
- **Secular ejecta** ($t > t_{dyn}$):
  - **neutrino-driven wind**
  - **MHD-viscosity-driven wind**

The ejecta expands homologously with density and radial velocity profile:

$$\rho_{\rm ej}(r < R_{\rm ej}, t) \propto \frac{M_{\rm ej}(t)}{R_{\rm ej}^3(t)} \left[\frac{r}{R_{\rm ej}(t)}\right]^{-k}, \; (k < 3) \qquad R_{\rm ej} = \beta_{\rm max} c\, t$$

$$\beta_{\rm ej}(r < R_{\rm ej}, t) = \beta_{\rm max} \left(\frac{r}{R_{\rm ej}(t)}\right)$$

Jet breakout time

The relativistic jet is slowed down by the confining medium. It inflates a cocoon that collimates it.
(Matzner '03; Bromberg+11; Murguia-Berthier+14; Matsumoto & Kimura '18; Lazzati & Perna '19)

$$\beta_h = \frac{\beta_j + \tilde{L}^{-1/2}\beta_{\rm ej}}{1+\tilde{L}^{-1/2}} \qquad \tilde{L} \simeq \frac{L_j}{\Sigma_j \rho_{\rm ej} c^3}$$

(RG, Nathanail, Rezzolla '19)

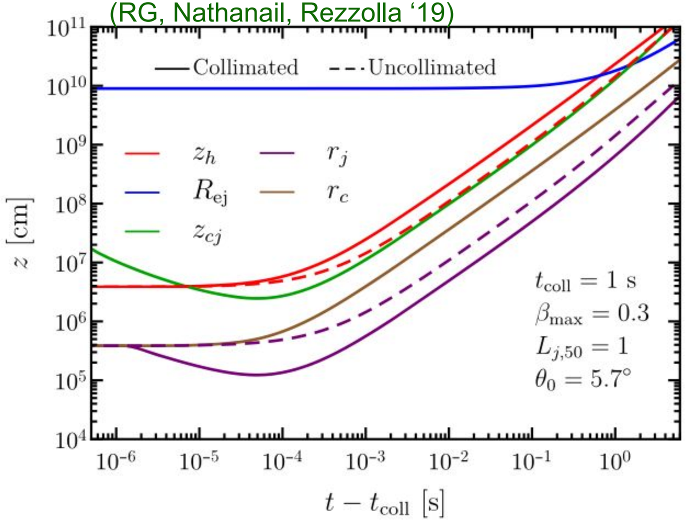

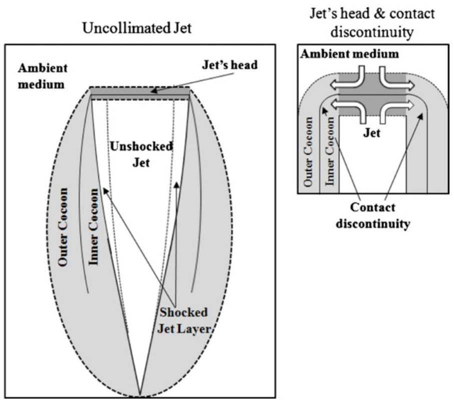

(Bromberg+2011)

More detailed and simulation calibrated analytic works find some differences with this simple treatment:

(Lyutikov '20; Margalit+18; Hamidani+20; Hamidani & Ioka '21; Gottlieb & Nakar '22; ….)

Jet breakout time inferred from the plateaus seen in the duration distribution of short GRBs suggests: (Mohrana & Piran '17)

$$t_{\rm bo} \sim 0.4\,{\rm s}$$

Radial and angular time delay

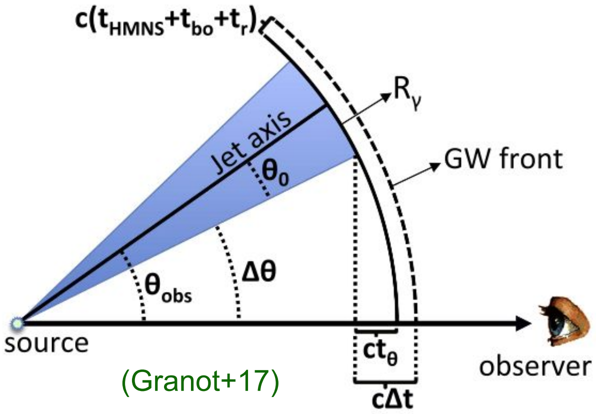

(Granot+17)

Additional time delay is caused by the slower than light expansion speed of the jet and light travel time effects:

Radial delay: $t_R \simeq \frac{R_\gamma}{2\Gamma^2 c} = 1.7\, R_{\gamma,13}\, \Gamma_{2.5}^{-2}\, \mathrm{ms}$

Angular delay: $t_\theta = \frac{R_\gamma}{c}[1 - \cos\Delta\theta] \simeq \frac{R_\gamma}{2c}(\Delta\theta)^2 = 1.67\, R_{\gamma,13}\, \Delta\theta_{-1}^2\, \mathrm{s}$

Total delay: $t_\gamma = t_R + t_\theta \simeq \frac{R_\gamma}{2c}\left[\frac{1}{\Gamma^2} + (\Delta\theta)^2\right]$

Different emission radii:

- Shock-breakout from fast tail
- Photospheric radius
- Internal shock radius: $R_{\mathrm{IS}} = 2\Gamma^2 c\, t_v \simeq 6 \times 10^{12}\, \Gamma_2^2\, t_{v,-2}\, \mathrm{cm}$

Emission radius from pulse width:

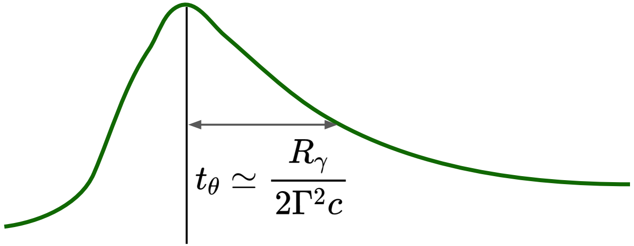

GW170817/GRB 170817A

LVC + Fermi + INTEGRAL ‘17

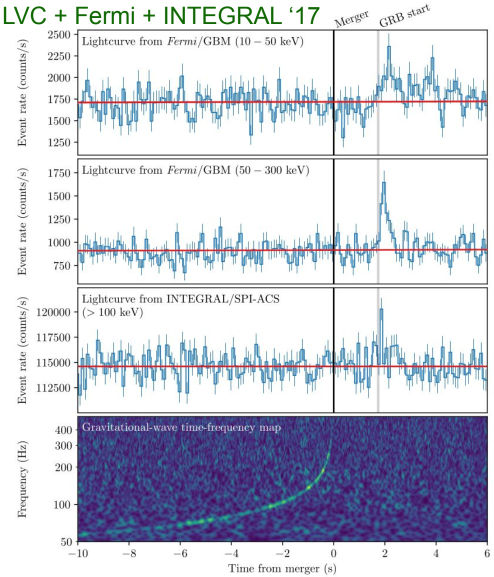

In GW170817, the prompt gamma-ray photons arrived after the GWs with a delay:

$$t_{\rm del} = 1.74 \pm 0.05\,{\rm s}$$

The observer was off-axis $(\theta_{\rm obs} \sim 20^{\circ})$ but saw emission from material along the line-of-sight:

- Subluminous prompt emission
- Shallow rise of afterglow lightcurve

(Lazzati+18)

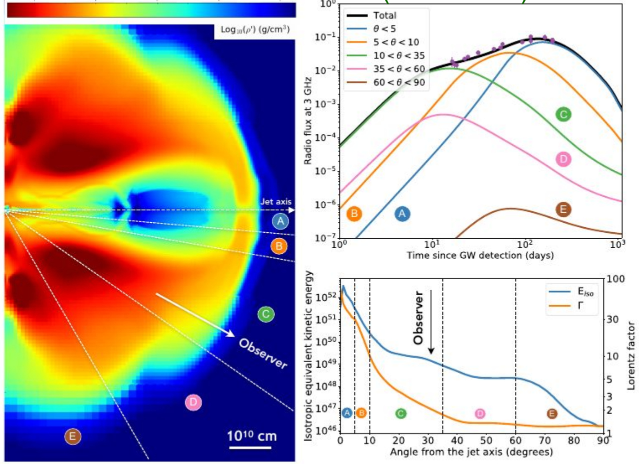

Merger remnant did not promptly collapse to a BH:

- $M_{\rm tot} = 2.74 M_{\odot} < M_{\rm th} = 2.82 M_{\odot}$
- Cannot produce “blue” ejecta mass and high electron fraction

Merger remnant collapse time

The delay time was used to constrain the collapse time of the merger remnant:

(RG, Nathanail, Rezzolla ‘19)

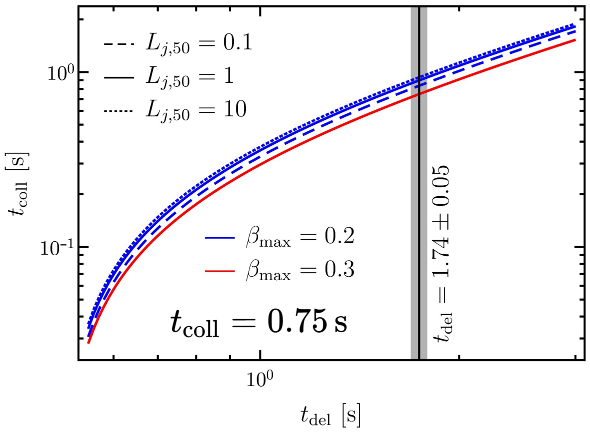

(Lazzati, Ciolfi, Perna 2020)

Model	$\Delta t_{\rm m-j}$ (s)	η	$\theta_{\rm l.o.s}$ (°)	$\theta_{\rm j}$ (°)
Simulations; baseline ($Y_e = 0.5$; $\Gamma_{\rm l.o.s.} \leqslant 10$; $m_{\rm w}$ unconstrained)	**<0.36**	**>240**	$\mathbf{23.5^{+5.5}_{-4.5}}$	$\mathbf{17.9^{+12.6}_{-3.2}}$
Simulations; $\Gamma_{\rm l.o.s.} \leqslant 7$	<0.18	>240	$24^{+6.9}_{-3.5}$	$18.4^{+12.5}_{-3.1}$
Simulations; $m_{\rm w} \geqslant 10^{-2}$	<0.37	>390	$23.6^{+4.8}_{-4.5}$	$17.3^{+13.4}_{-2.5}$
Simulations; $\Gamma_{\rm l.o.s.} \leqslant 7$; $m_{\rm w} \geqslant 10^{-2}$	<0.17	>250	$24.1^{+6.7}_{-3.6}$	$19.3^{+11.9}_{-3.9}$
Parametric; baseline ($Y_e = 0.5$; $\Gamma_{\rm l.o.s.} \leqslant 10$; $m_{\rm w}$ unconstrained)	**<1.1**	**>150**	$\mathbf{30.3^{+8.5}_{-8.0}}$	$\mathbf{10.2^{+8.8}_{-3.0}}$
Parametric; $\Gamma_{\rm l.o.s.} \leqslant 7$	<0.87	>180	$34.4^{+6.4}_{-8.6}$	$9.2^{+9.7}_{-1.8}$
Parametric; $m_{\rm w} \geqslant 10^{-2}$	<0.87	>420	$27.5^{+6.0}_{-7.1}$	$16.2^{+11.3}_{-3.2}$
Parametric; $\Gamma_{\rm l.o.s.} \leqslant 7$; $m_{\rm w} \geqslant 10^{-2}$	<0.57	>800	$30.7^{+6.2}_{-6.8}$	$16.3^{+13.8}_{-1.2}$

(Hamidani, Kiuchi, Ioka 2019)

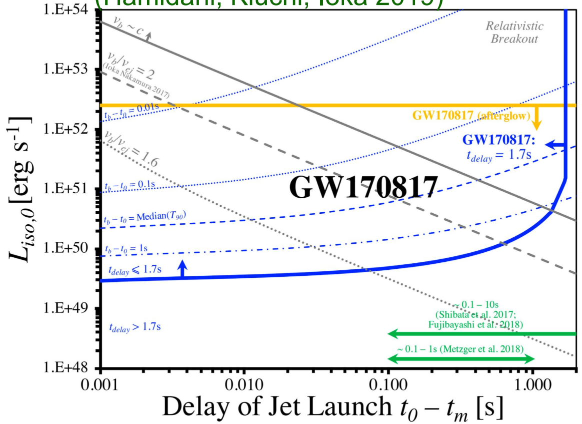

Several works found broadly consistent results, but no strong constraints on the collapse time due to several model uncertainties.

Afterglow Polarization

Afterglow shocks & linear polarization

Afterglow shocks are collisionless that accelerate particles into a power-law energy distribution and amplify/generate small-scale B-fields. The particles cools by radiating synchrotron photons.

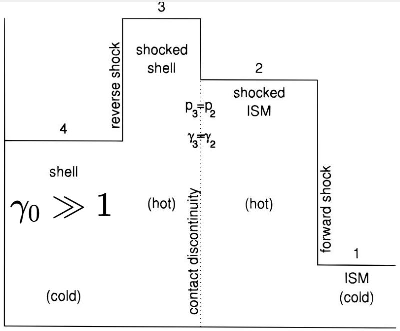

(Sari, Narayan, Piran 1996)

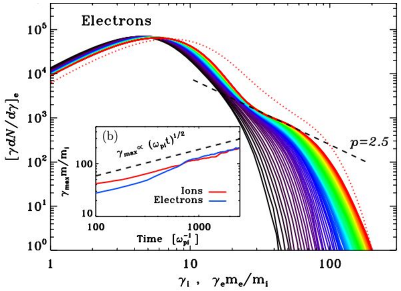

(Sironi, Spitkovsky, Arons 2013)

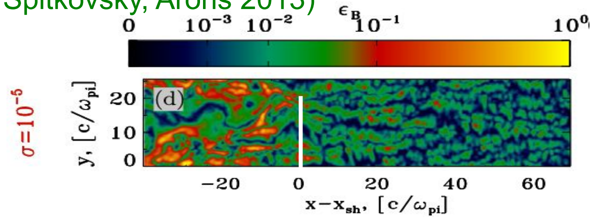

Optical polarimetery of GRB afterglows finds:

- P ~ few x 10% during the **reverse-shock** dominated afterglow (early times)
- P ~ few % during the **forward-shock** dominated afterglow (late times)

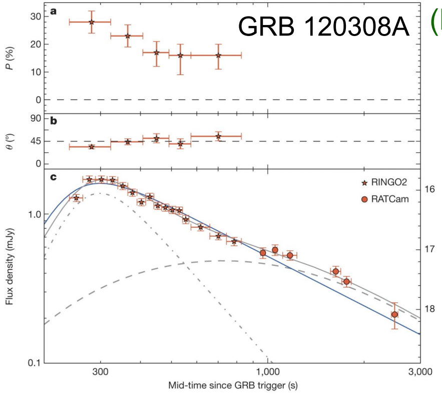

(Mundell+2013)

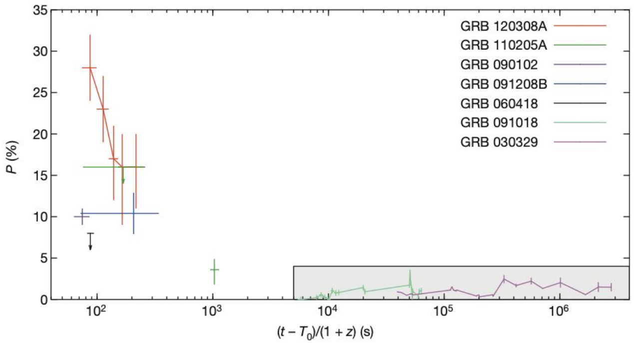

Magnetic field structure

$B_\perp$: small-scale ($\Gamma\theta_B \ll 1$) field generated by streaming instabilities;
- confined to the plane transverse to the shock normal
(Medvedev & Loeb '99; Gruzinov '99; Sari '99; Granot & Konigle '03)

$B_\parallel$: ordered field aligned along the local shock normal
(Gruzinov '99; Sari '99; Granot & Konigle '03)

|P| > 0 is obtained when symmetry of image is broken:

(a) off-axis observer 'sees' jet edge **(b) jet angular structure**

$B_\perp$

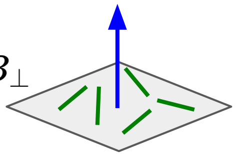

$B_\parallel$

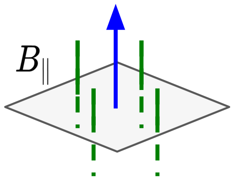

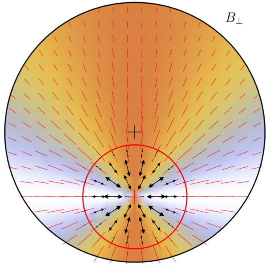

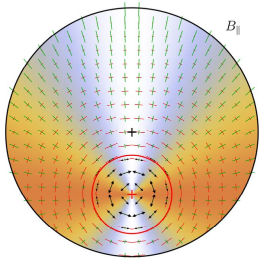

$B_{\rm tor}$: globally ordered toroidal field symmetric around the jet axis
(naturally arises in a high-magnetization outflow)
(Lyutikov+03; Granot & Taylor '05)

$B_{\rm ord}$: ordered field within a radiating patch with coherence length larger than the beaming cone: $1/\Gamma \leq \theta_B \ll \theta_j$ (Gruzinov & Waxman '99)

$B_{\rm tor}$

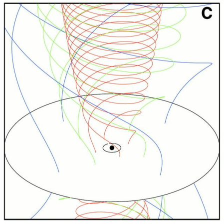

(Meier+01)

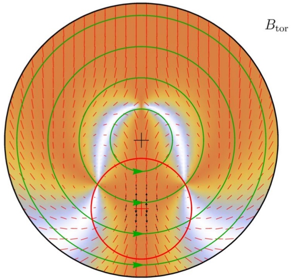

Forward-shock afterglow polarization

Ignoring the (post-shock) radial structure, polarization is calculated for a prescribed level of B-field anisotropy:
(Gruzinov & Waxman '99; Gruzinov '99; Ghisellini & Lazzati '99; Sari '99; Granot & Konigl '03; Rossi+04)

$$b \equiv \frac{2\langle B_{\parallel}^2\rangle}{\langle B_{\perp}^2\rangle} \qquad \frac{\Pi_{\rm local}(\theta')}{\Pi_{\rm max}} = \frac{(b-1)\sin^2\theta'}{2+(b-1)\sin^2\theta'}$$

Afterglow modeling of GRB 170817A with a power-law structured jet removed the degeneracy!

Non-spreading top-hat jet (Rossi+04)

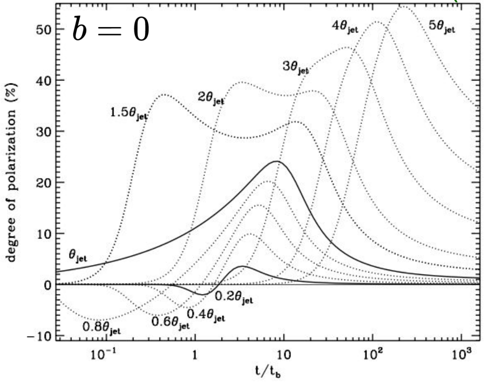

Non-spreading power-law structured jet

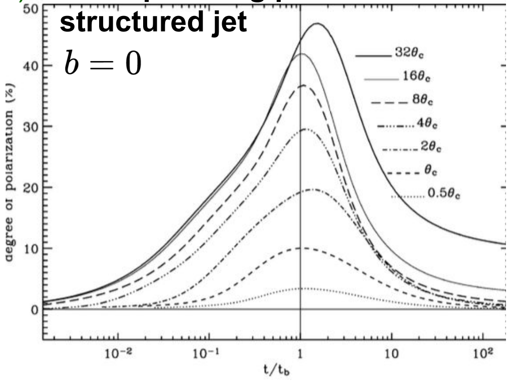

(Corsi+18)

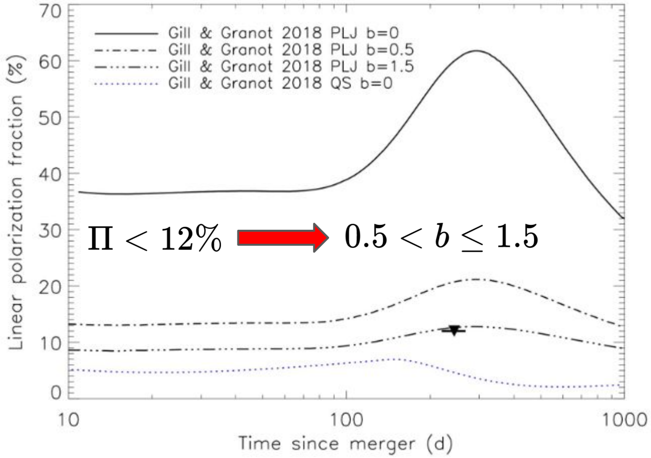

The value of b can only be constrained for a given jet structure and viewing geometry

Constraint on post-shock B-field anisotropy

Including the radial structure of the post-shock flow allows to constrain the B-field anisotropy just behind shock: (RG & Granot 2021)

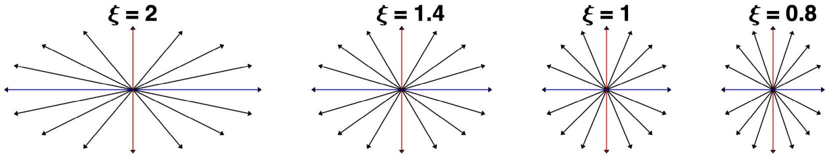

$$\chi = 1 + 2(4-k)\Gamma_{\rm sh}^2(1 - r/R) \qquad \chi = 1$$

$$\xi(\chi) = \frac{B_\parallel(\chi)}{B_\perp(\chi)} = \xi_f \chi^{(7-2k)/(8-2k)} \qquad n_{\rm ext} \propto R^{-k}$$

Due to radial stretching of fluid elements, the radial B-field component becomes dominant

Post-shock B-field is more isotropic than anisotropic:

$$0.6 \leq \xi_f \leq 0.9 \qquad 0.7 \leq b \leq 1.5$$

(Granot & Konigl '03; Stringer & Lazzati '20)

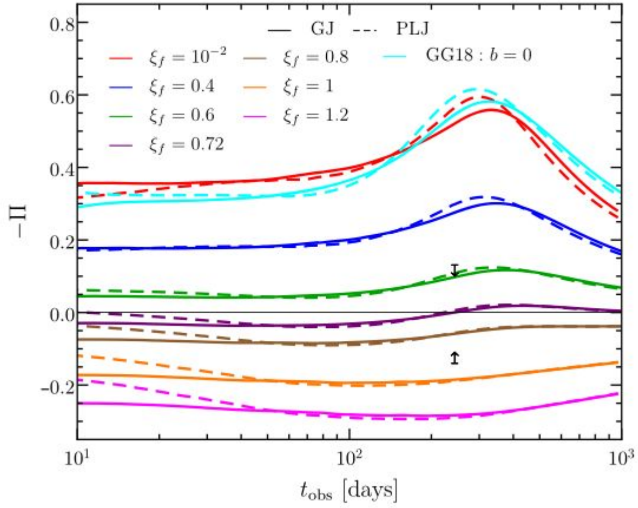

Macroscopic turbulence at the shock front can yield a more isotropic field (Sironi & Goodman '07; Couch+08; Zhang+09)

Optical polarimetry of GRB 180720B

(Arimoto+2024)

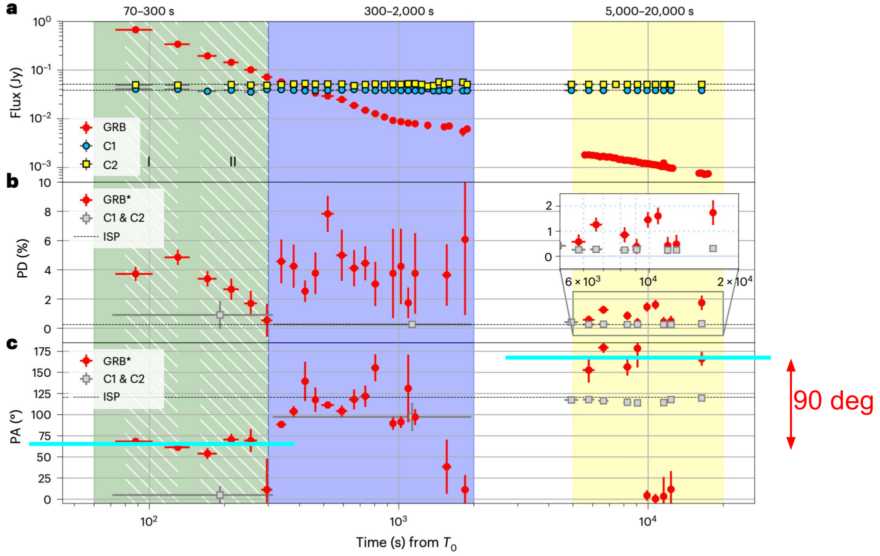

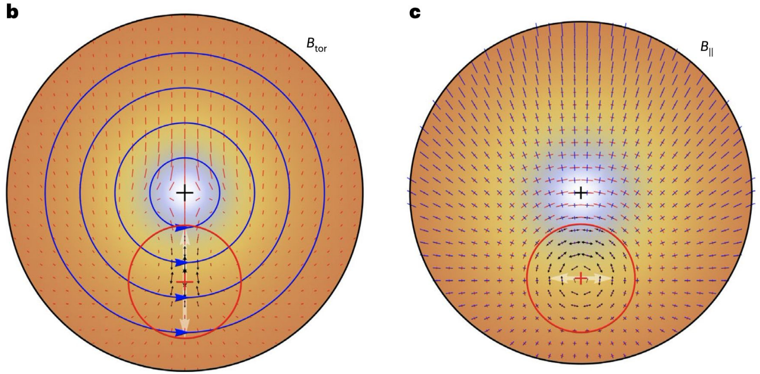

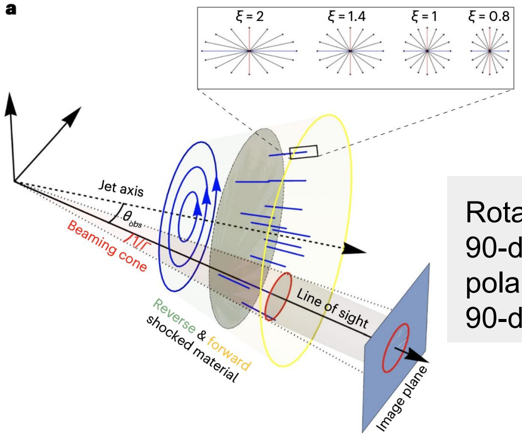

GRB polarization is obtained after removing any induced polarization en route

$$\hat{\Pi} = \hat{n} \times \hat{B}$$

Rotation of B-field by 90-deg also rotates the polarization vector by 90-deg

Summary & Conclusions

The time delay between reception of GWs and gamma-rays from both long-soft and short-hard GRBs can be instrumental in constraining the **properties of the remnant**, **jet propagation in the respective confining media**, and **jet breakout physics**.

There are **still a lot of holes in our understanding jet propagation inside expanding ejecta** and where the gamma-ray emission is generated in jets in short-hard GRBs - shock breakout or internal dissipation?

Afterglow polarization a is valuable tool **for understanding the magnetic field structure in collisionless shocks** and for probing the jet composition.

The prediction of highly anisotropic B-field just behind the shock, which is also obtained in PIC simulations, is at odds with constraints obtained low afterglow polarization measurements, that suggest more mixed B-field components.